Clumped isotope evidence for microbial alteration of thermogenic methane in terrestrial mud volcanoes

Jiarui Liu[1,*], Tina Treude[1,2], Orhan R. Abbasov[3], Elnur E. Baloglanov[3], Adil A. Aliyev[3], Carolynn M. Harris[4], William D. Leavitt[4,5], and Edward D. Young[1]

[1]Department of Earth, Planetary, and Space Sciences, University of California, Los Angeles, California 90095, USA
[2]Department of Atmospheric and Oceanic Sciences, University of California, Los Angeles, California 90095, USA
[3]Institute of Geology and Geophysics, Ministry of Science and Education, Baku AZ1143, Azerbaijan
[4]Department of Earth Sciences, Dartmouth College, Hanover, New Hampshire 03755, USA
[5]Department of Chemistry, Dartmouth College, Hanover, New Hampshire 03755, USA

ABSTRACT

Methane in oil reservoirs originates mostly from thermogenic sources, yet secondary microbial methane production from petroleum biodegradation is known to be pervasive. The conventional approach for identifying this secondary microbial methane commonly relies on geochemical characteristics of other gas molecules such as the carbon isotopic composition of carbon dioxide and propane. This information is sometimes obscured by isotopic variations in source material and may not be available in certain geological reservoirs. To better constrain the presence of secondary microbial methane, we studied the clumped isotopologue compositions of methane in terrestrial Azerbaijanian mud volcanoes, which support the occurrence of secondary microbial gas. Here, a deficit in $\Delta^{12}CH_2D_2$ of thermogenic methane occurs due to different δD of hydrogen sources that contribute to the formation of methane molecules (i.e., combinatorial effect). The $\Delta^{12}CH_2D_2$ is expected to move toward equilibrium as thermal maturity increases. More importantly, both $\Delta^{13}CH_3D$ and $\Delta^{12}CH_2D_2$ values of methane approach low-temperature thermodynamic equilibrium in most gases, suggesting that the original thermogenic methane has been altered by newly formed microbial methane in addition to isotope exchange among methane molecules catalyzed by the methyl-coenzyme M reductase enzyme. We conclude that methane clumped isotopes provide a unique proxy for identifying secondary microbial methane and understanding the exact evolution stages for natural gases.

INTRODUCTION

Methane is the simplest of all hydrocarbons and the main constituent of natural gas. Naturally occurring methane derives from three main sources: microbial, thermogenic, and abiotic. Microbial and thermogenic methane are formed by microbial degradation and thermocatalytic decomposition of organic matter, respectively (e.g., Reeburgh, 2007). Primary microbial gas forms from dispersed organic matter in relatively shallow sediments, whereas secondary microbial gas is produced from petroleum accumulations during biodegradation (e.g., Milkov, 2011). Abiotic methane is generated by magmatic and gas-water-rock reactions such as serpentinization and Sabatier reaction (e.g., Etiope and Sherwood Lollar, 2013).

The origins of methane are commonly inferred using diagrams plotting molecular ratios of alkanes against the bulk carbon and hydrogen isotopic composition of methane (Bernard et al., 1977; Whiticar, 1999). The fields indicating the methane sources in these empirical bivariate diagrams may overlap because bulk isotopic ratios reflect a combination of formation and alteration processes coupled with mixing and migration. For example, secondary microbial gas is commonly mixed with the original thermogenic gas in natural gas reservoirs, whereas their bulk isotopic compositions are almost indistinguishable (e.g., Milkov and Etiope, 2018). Given the complexity of bulk isotopic systematics of methane, an integrated geochemical-geological approach, including geochemical characteristics of associated gas molecules, is commonly used to recognize the presence of secondary microbial gas (Milkov, 2011, and references therein).

During petroleum biodegradation, both short- and long-chain alkanes can be converted to methane. This methanogenic degradation can proceed either through syntrophic partnerships of hydrocarbon-degrading bacteria and methanogenic archaea (e.g., Zengler et al., 1999) or by alkylotrophic methanogenic archaea (Zhou et al., 2022). As biodegradation continues, the gas becomes more methane dominated with high $C_1/(C_2 + C_3)$ ratios, where C_1 is methane, C_2 is ethane, and C_3 is propane. In addition, as CO_2 derived from biodegraded petroleum is progressively converted into methane through the syntrophic pathway, the residual CO_2 becomes more enriched in ^{13}C, with $\delta^{13}C$ values commonly exceeding $+2‰$ and as high as $+36‰$ (Milkov and Etiope, 2018). This ^{13}C enrichment of CO_2 is considered to be one of the best geochemical indicators of secondary microbial gas (Etiope et al., 2009b; Milkov, 2011). As Etiope et al. (2009b) also pointed out, however, $\delta^{13}C_{CO2}$ variability can be more than $50‰$ within the same seepage system, both in space and time, suggesting that the $\delta^{13}C$ of CO_2 may be affected by environmental conditions such as isotopic variations in source material and/or extent of CO_2 conversion to methane. Similarly, ^{13}C-enriched propane has been used as a tracer of anaerobic biodegradation, but propane concentrations are commonly below detection limits in many natural gas reservoirs (Etiope et al., 2009b; Milkov, 2011).

To better identify the presence of secondary microbial methane, we focus on the multiply substituted, a.k.a. "clumped," isotopologue compositions of methane. In general, isotope clumping, or isotopic bond ordering, traces the processes controlling the formation of the molecules independent of source material (Stolper et al., 2014; Wang et al., 2015; Young et al.,

Jiarui Liu [ORCID] https://orcid.org/0000-0003-4878-6578
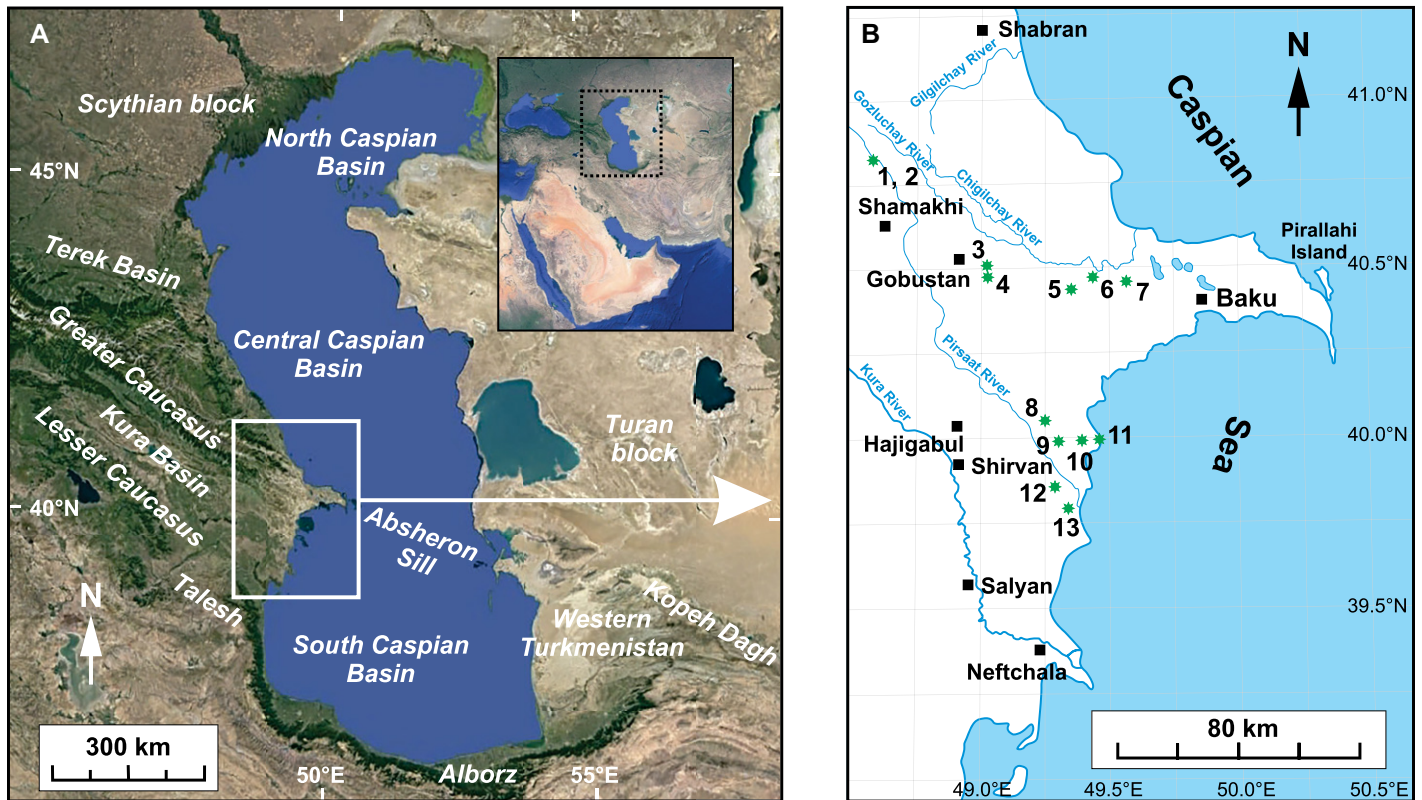*jiaruiliu@ucla.edu

Figure 1. Location map of sampled mud volcanoes. (A) Satellite maps of the Caspian Sea and surrounding geological features (Google Earth). Inset places the enlargement within the wider West and Central Asia. (B) Map of sampled mud volcanoes in eastern Azerbaijan (Aliyev et al., 2015). Green asterisks represent sampled mud volcanoes 1–13 as detailed in Table 1. White box in map A shows location of map B.

2017). The combination of two mass-18 methane isotopologues ($^{13}CH_3D$ and $^{12}CH_2D_2$) of thermogenic methane commonly records equilibrium at its formation temperature of ∼100–250 °C (e.g., Stolper et al., 2014; Young et al., 2017; Xie et al., 2021). Microbially produced methane, on the other hand, shows disequilibrium signatures or approaches equilibrium at an ambient temperature of ∼0–80 °C (e.g., Wang et al., 2015; Young et al., 2017; Taenzer et al., 2020). Therefore, we would expect distinct clumped isotope signatures of secondary microbial methane different from those of the original thermogenic gas (cf. Giunta et al., 2019; Thiagarajan et al., 2020; Jautzy et al., 2021; Zhang et al., 2021; Lalk et al., 2022). To further our understanding of natural gas evolution, we analyzed the isotopologue ratios of methane from terrestrial mud volcanoes in Azerbaijan, where methanogenic biodegradation has been proposed based on simulated petroleum seepage experiments and the presence of ^{13}C-enriched CO_2 and propane (Etiope et al., 2009b; Mishra et al., 2017).

STUDY AREA AND METHODOLOGY

Mud volcanoes are constructional features from which sediments and fluids flow or erupt, acting as an important source of methane to the atmosphere and to the ocean (e.g., Etiope et al., 2004). The most active terrestrial area with the

highest number of mud volcanoes is located in eastern Azerbaijan (Aliyev et al., 2015). We sampled gas and liquid mud separately from 13 mud volcanoes across different tectonic blocks in eastern Azerbaijan (Fig. 1; Figs. S1–S2 in the Supplemental Material[1]). Their geochemical characteristics were analyzed using standard methods (see the Supplemental Material), including gas compositions, isotopologue ratios of methane, $\delta^{13}C$ of CO_2, and δD of water. The relative abundances of the two mass-18 isotopologues are presented in standard Δ notation (Fig. 2A), representing deviations from a stochastic standard in which distributions of isotopes across all isotopologues are effectively random (Young et al., 2017).

CLUMPED ISOTOPE SIGNATURE OF THERMOGENIC METHANE FROM MUD VOLCANOES

Methane gas from mud volcanoes mostly originates from thermogenic sources in the deep subsurface (Etiope et al., 2009a). However, only one out of the 13 sampled mud volcanoes in the study area released typical ther-

---

[1]Supplemental Material. Geological background, supplemental methods, and Figures S1–S4. Please visit https://doi.org/10.1130/GEOL.S.24328633 to access the supplemental material; contact editing@geosociety.org with any questions.

mogenic methane as inferred using diagrams shown in Figures 2B–2D and Figure S3. This thermogenic gas, sampled from the Aghzybir mud volcano (location 13 in Fig. 1), has a low $C_1/(C_2 + C_3)$ ratio of 19 as a result of high abundances of ethane and propane, though its bulk $\delta^{13}C$ and δD are indistinguishable from those of the rest of the gases (Table 1). The clumped isotope composition of this methane sample exhibits a pronounced disequilibrium isotopologue signature with a low $\Delta^{12}CH_2D_2$ value (Fig. 2A). Recent studies demonstrate that $\Delta^{13}CH_3D$ values of thermogenic methane gases are consistent with thermodynamic equilibrium at their formation temperatures (Dong et al., 2021; Xie et al., 2021). The authors of these studies found that, however, a deficit in $\Delta^{12}CH_2D_2$ in thermogenic methane can occur due to significantly different δD of hydrogen sources that contribute to the formation of methane molecules (i.e., combinatorial effect). The departure from equilibrium is most pronounced at low thermal maturities, and the $\Delta^{12}CH_2D_2$ moves toward equilibrium as maturity increases (Xie et al., 2021). This deficit in $\Delta^{12}CH_2D_2$ is observed in the Aghzybir gas, while its $\Delta^{13}CH_3D$ value (3.9‰ ± 0.2‰) corresponds to an apparent formation temperature of 100 ± 8 °C. This temperature is lower than the peak thermogenic gas window (170–180 °C) but still within the nominal gas
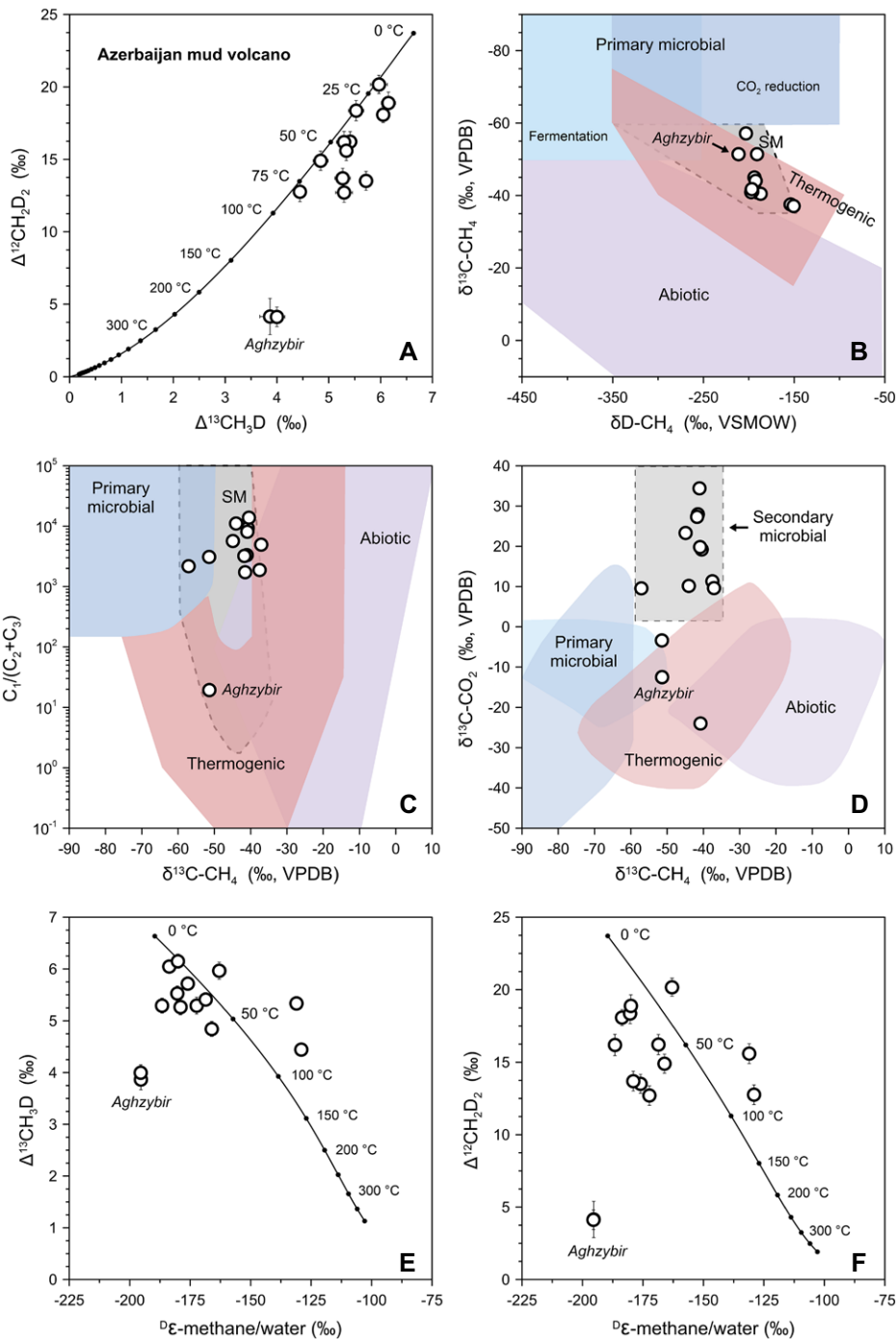
Figure 2. **Genetic diagrams of mud volcano gases from Azerbaijan. (A) Clumped isotope data of methane. Solid black line depicts theoretical thermodynamic equilibrium abundances of methane isotopologues, along with corresponding temperatures. (B) Bulk isotope data of methane. (C) $\delta^{13}C_{CH4}$ versus $C_1/(C_2 + C_3)$. (D) $\delta^{13}C_{CH4}$ versus $\delta^{13}C_{CO2}$. Genetic fields in panels B–D follow Bernard et al. (1977), Whiticar (1999), and Milkov and Etiope (2018). Secondary microbial (SM) field is shown in gray with dashed line. (E–F) $\Delta^{13}CH_3D$ and $\Delta^{12}CH_2D_2$ versus hydrogen isotope fractionation ($^D\varepsilon$) between methane and associated environmental water (cf. Wang et al., 2015). Solid black curve represents thermodynamic isotopic equilibrium, with the $\varepsilon_{methane/water}$ calibration given by Turner et al. (2022). Aghzybir mud volcano is the only one releasing typical thermogenic methane. Error bars are one standard error. VPDB—Vienna Peedee belemnite; VSMOW—Vienna standard mean ocean water.**

MICROBIAL ALTERATION OF THERMOGENIC METHANE

Except for the Aghzybir mud volcano, all the remaining sampled mud volcanoes release methane-dominated gas with high $C_1/(C_2 + C_3)$ ratios on the order of 10^3 to 10^4 (Fig. 2C). In particular, the propane (C_3) and n-butane (n-C_4) concentrations in these gases are near or below detection limits (7.9 $\pm$ 11.9 and 0.3 $\pm$ 1.2 ppm, respectively), whereas the average iso-butane (i-C_4) concentration is 29.3 $\pm$ 11.5 ppm (Table 1). These gas compositions are consistent with anaerobic degradation of propane and n-butane by microorganisms. Microbial ecosystems documented in marine hydrocarbon seeps can oxidize propane and n-butane simultaneously but not iso-butane (e.g., Kniemeyer et al., 2007). Furthermore, most of these gases are associated with ^{13}C-enriched CO_2 (Fig. 2D), supporting the hypothesis of coupled hydrocarbon degradation and secondary methanogenesis (Etiope et al., 2009b). In addition to biodegradation, molecular fractionation during migration further leads to systematic loss of heavy hydrocarbons from reservoir to surface in mud volcanoes where gas migration is dominated by advection but not diffusion (Etiope et al., 2009a). Accordingly, isotope fractionation may occur during transportation but is generally not significant (Etiope et al., 2009a, 2009b).

The $\Delta^{13}CH_3D$ and $\Delta^{12}CH_2D_2$ values of biodegraded gases range from 4.4‰ to 6.1‰ and from 12.7‰ to 20.2‰, respectively, corresponding to apparent temperatures of 13–75 °C and 21–83 °C, respectively (Fig. 2A). In plots of $\Delta^{13}CH_3D$ versus $\Delta^{12}CH_2D_2$, methane from four samples plot on the thermodynamic equilibrium curve, yielding equilibrium temperatures of ~20, 33, 59, and 79 °C. The lowest temperature of 20 °C inferred from the Khydyrly gas is consistent with the measured in situ liquid temperature of 21 $\pm$ 4 °C at the surface (Table 1). The clumped isotopologue ratios, therefore, suggest that isotopic bond ordering in the original higher-temperature thermogenic methane has been modified by microbial activity at lower temperatures, resulting in methane equilibrated at the low ambient temperatures. Therefore, methane seeping from these mud volcanoes is a mixture of thermogenic and its equivalent biodegraded methane, the latter being the result of low-temperature microbial methanogenesis. With burial, the evolution of isotopic bond ordering in thermogenic gas from low to high maturity occurs at temperatures >100 °C (e.g., 175 °C; Xie et al., 2021). Accordingly, we assume that the $\Delta^{12}CH_2D_2$ increases from negative values (e.g., −25‰ at early thermal maturity) to equilibrium values (e.g., +7‰) for the thermogenic end member. Subsequently, uplift and/or migration allow biodegradation to occur at lower temperatures. The microbial end member corresponds to thermodynamic equilibrium

window (e.g., Stolper et al., 2014). In addition, the δD offset between methane and water is 192‰ in the Aghzybir mud volcano, significantly higher than the equilibrium prediction

of 136‰ $\pm$ 2‰ at 100 $\pm$ 8 °C (Turner et al., 2022), which further confirms hydrogen isotope disequilibrium between methane and groundwater (Figs. 2E–2F).

TABLE 1. ISOTOPIC RATIO, GAS COMPOSITION, AND IN SITU TEMPERATURE OF LIQUID MUD (T_{LIQUID}) OF SAMPLES FROM AZERBAIJAN MUD VOLCANOES

Location	$\delta^{13}C_{CH4}$ (‰, VPDB)	δD_{CH4} (‰, VSMOW)	$\Delta^{13}CH_3D$ (‰)	$\Delta^{12}CH_2D_2$ (‰)	$C_1/$ $(C_2 + C_3)$	C_3 (ppm)	i-C_4 (ppm)	n-C_4 (ppm)	$\delta^{13}C_{CO2}$ (‰, VPDB)	δD_{H2O} (‰, VSMOW)	T_{liquid} (°C)
1. Demirchi (gray)	−37.1	−150.7	4.4	12.8	4948	5	35	0	9.6	−24.8	14
2. Demirchi (brown)	−37.5	−153.9	5.3	15.6	1874	18	33	0	11.3	−26.3	12
3. Kichik Mereze	−40.9	−197.2	6.1	18.9	8052	0	37	0	19.8	−21.0	23
4. Shikhzarli	−40.5	−186.8	5.4	16.2	13,831	0	25	0	19.2	−22.0	25
5. Garyja	−41.8	−196.7	5.3	13.7	3219	14	38	4	27.3	−21.6	18
6. Pirekeshkul	−41.6	−197.0	5.3	16.2	1729	5	24	0	28.0	−12.7	21
7. Uchtepe	−41.1	−196.1	5.5	18.4	3302	0	34	0	34.4	−19.3	22
8. Solakhay	−57.1	−203.1	6.0	18.1	2176	41	46	0	9.6	−23.8	22
9. Ayrantoken	−45.0	−193.7	5.7	13.5	5683	7	38	0	23.3	−21.5	21
10. Dashgil	−40.8	−190.1	4.8	14.9	9279	5	18	0	−24.0	−28.8	22
11. Bahar	−44.0	−192.3	5.3	12.7	11,043	0	5	0	10.2	−24.2	25
12. Khydyrly	−51.4	−190.8	6.0	20.2	3096	0	19	0	−3.4	−33.3	26
13. Aghzybir	−51.4	−211.3	4.0	4.1	19	14,865	3240	3063	−12.5	−19.7	25
	−51.4	−211.2	3.9	4.1	19	14,993	3271	3207			

Note: C_1—methane; C_2—ethane; C_3—propane; i-C_4—iso-butane; n-C_4—n-butane. Note that two mud volcanoes were sampled near Demirchi village, one with gray liquid mud, the other with brown liquid mud. Two subsamples from the Aghzybir mud volcano were measured for methane isotopologue ratio and alkane composition, as shown in the bottom two rows. VPDB—Vienna Peedee belemnite; VSMOW—Vienna standard mean ocean water.

at 12 °C, the lowest measured in situ liquid temperature (Table 1). Mixing between these end members, therefore, encompasses all the mud volcano data (Fig. 3).

The isotopologue signature of microbial methane found here is different from that from laboratory culture studies and many terrestrial settings where significant clumped isotope disequilibrium is observed (Wang et al., 2015; Young et al., 2017). Recent studies demonstrate that the kinetic isotope effects and associated combinatorial effects are expressed when the reversibility of intracellular reactions is low (e.g., laboratory culture), leading to disequilibrium isotopologue signals (Cao et al., 2019; Young, 2019; Gropp et al., 2022; Ono et al., 2022). In energy-limited deep sedimentary environments with higher reaction reversibility (e.g., mud volcano), however, enzymatically mediated exchange of isotopes among methane molecules is evidently more pronounced, translating into near-equilibrium isotopologue signatures (Gropp et al., 2022; Ono et al., 2022). Thus, the observed isotopologue values (Fig. 2A) are consistent with these model predictions. Among all the intracellular pathways, the last step of microbial methanogenesis catalyzed by the methyl-coenzyme M reductase (Mcr) enzyme is evidently central to the mechanism for isotopologue equilibration. Recent experiments demonstrated that the headspace methane approaches isotopologue equilibration during isotope exchange solely with the Mcr enzyme (Liu et al., 2023). Accordingly, in addition to the generation of newly formed secondary microbial methane, this Mcr-catalyzed isotope exchange promotes isotopic bond reordering within the original thermogenic methane, both contributing to the observed low-temperature thermodynamic equilibrium (Fig. 2A). Indeed, the microbially altered methane appears to approach hydrogen isotope equilibrium with associated waters at or near the temperatures indicated by the $\Delta^{13}CH_3D$ and $\Delta^{12}CH_2D_2$ data (Figs. 2E–2F), suggesting the occurrence of both intra- and inter-species isotope equilibrium.

Once formed, methane could be oxidized by anaerobic methanotrophic (ANME) archaea in the subsurface. Indeed, ANME archaea have been reported in terrestrial mud volcanoes and nearby sediment across the globe, including the ones studied here (Alain et al., 2006; Stagars et al., 2017; Lin et al., 2018). Because anaerobic oxidation of methane (AOM) is the enzymatic reversal of major methanogenic pathways, the principle of the clumped isotopologue effect during AOM is broadly similar to that of methanogenesis, meaning isotopologue equilibration under energy-limited conditions (Young et al., 2017; Ash et al., 2019; Ono et al., 2022; Liu et al., 2023). Given the potential occurrence of simultaneous methane production and consumption, we generalized the near-equilibrium methane isotopologue signatures as a result of the Mcr-catalyzed intracellular isotope exchange operating under near-threshold free-energy conditions in the deep biosphere.

CONCLUSIONS

Using terrestrial Azerbaijanian mud volcanoes as an example, we demonstrate that the original thermogenic methane gas is augmented by methane formed during methanogenic hydrocarbon biodegradation. The clumped isotopic ratios of this secondary microbial methane ultimately approach low-temperature thermodynamic equilibrium, whereas primary microbial methane emissions exhibit notable clumped iso-
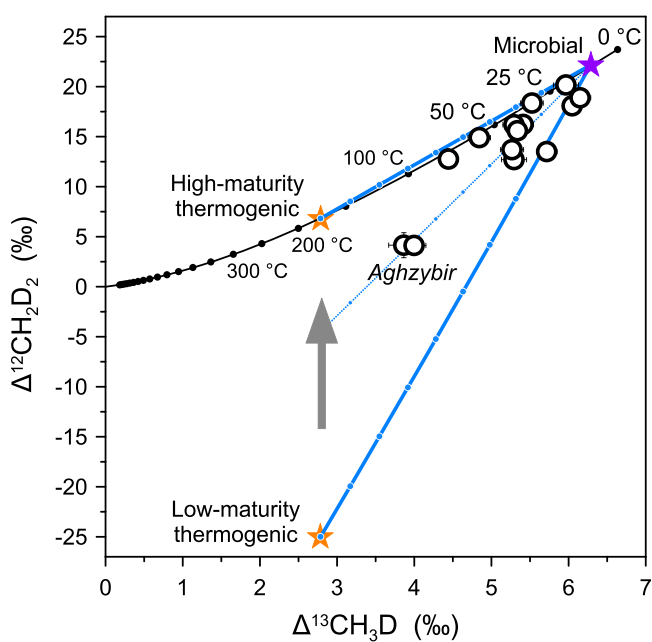

Figure 3. **Schematic illustration of clumped isotope evolution of methane in natural gas reservoirs. Two orange stars and gray arrow depict evolution of thermogenic methane from low to high maturity with formation temperature of 175 °C (Dong et al., 2021; Xie et al., 2021). Purple star represents a microbial end member at 12 °C (Table 1). Blue lines demonstrate three scenarios of mixing between thermogenic and low-temperature microbial end members with blue points marking 10% intervals of mixing. Measured bulk isotopic data are used for the calculation. In principle, mixing is nonlinear for multiply substituted isotopologues, whereas the mixing lines here are quasi-linear because the bulk isotopic compositions of the two end members are similar (Young et al., 2017). The solid black line depicts theoretical thermodynamic equilibrium abundances of methane isotopologues along with corresponding temperatures.**

tope disequilibrium (e.g., Young, 2019). Given that secondary methanogenesis significantly increases methane emissions into the atmosphere (Milkov, 2011), it is crucial to consider the role of secondary microbial methane in biological contributions to global isotopologue budgets. Overall, this independent approach offers a unique perspective for identifying secondary microbial gas and tracking the fate of methane in oil and gas reservoirs.

REFERENCES CITED
Alain, K., Holler, T., Musat, F., Elvert, M., Treude, T., and Krüger, M., 2006, Microbiological investigation of methane- and hydrocarbon-discharging mud volcanoes in the Carpathian Mountains, Romania: Environmental Microbiology, v. 8, p. 574–590, https://doi.org/10.1111/j.1462-2920.2005.00922.x.

Aliyev, A.A., Guliyev, I.S., Dadashev, F.G., and Rahmanov, R.R., 2015, Atlas of the world mud volcanoes: Baku, Nafta-Press Publishing House, Sandro Teti Editore, 361 p.

Ash, J.L., Egger, M., Treude, T., Kohl, I., Cragg, B., Parkes, R.J., Slomp, C.P., Sherwood Lollar, B., and Young, E.D., 2019, Exchange catalysis during anaerobic methanotrophy revealed by $^{12}CH_2D_2$ and $^{13}CH_3D$ in methane: Geochemical Perspectives Letters, v. 10, p. 26–30, https://doi.org/10.7185/geochemlet.1910.

Bernard, B., Brooks, J.M., and Sackett, W.M., 1977, A geochemical model for characterization of hydrocarbon gas sources in marine sediments: Paper OTC 2934, presented at 9th Annual Offshore Technology Conference, Houston, Texas, 2–5 May, p. 435–438, https://doi.org/10.4043/2934-MS.

Cao, X., Bao, H., and Peng, Y., 2019, A kinetic model for isotopologue signatures of methane generated by biotic and abiotic CO_2 methanation: Geochimica et Cosmochimica Acta, v. 249, p. 59–75, https://doi.org/10.1016/j.gca.2019.01.021.

Dong, G., Xie, H., Formolo, M., Lawson, M., Sessions, A., and Eiler, J., 2021, Clumped isotope effects of thermogenic methane formation: Insights from pyrolysis of hydrocarbons: Geochimica et Cosmochimica Acta, v. 303, p. 159–183, https://doi.org/10.1016/j.gca.2021.03.009.

Etiope, G., and Sherwood Lollar, B., 2013, Abiotic methane on Earth: Reviews of Geophysics, v. 51, p. 276–299, https://doi.org/10.1002/rog.20011.

Etiope, G., Feyzullayev, A., Baciu, C.L., and Milkov, A.V., 2004, Methane emission from mud volcanoes in eastern Azerbaijan: Geology, v. 32, p. 465–468, https://doi.org/10.1130/G20320.1.

Etiope, G., Feyzullayev, A., and Baciu, C.L., 2009a, Terrestrial methane seeps and mud volcanoes: A global perspective of gas origin: Marine and Petroleum Geology, v. 26, p. 333–344, https://doi.org/10.1016/j.marpetgeo.2008.03.001.

Etiope, G., Feyzullayev, A., Milkov, A.V., Waseda, A., Mizobe, K., and Sun, C.H., 2009b, Evidence of subsurface anaerobic biodegradation of hydrocarbons and potential secondary methanogenesis in terrestrial mud volcanoes: Marine and Petroleum Geology, v. 26, p. 1692–1703, https://doi.org/10.1016/j.marpetgeo.2008.12.002.

Giunta, T., et al., 2019, Methane sources and sinks in continental sedimentary systems: New insights from paired clumped isotopologues $^{13}CH_3D$ and $^{12}CH_2D_2$: Geochimica et Cosmochimica Acta, v. 245, p. 327–351, https://doi.org/10.1016/j.gca.2018.10.030.

Gropp, J., Jin, Q., and Halevy, I., 2022, Controls on the isotopic composition of microbial methane: Science Advances, v. 8, https://doi.org/10.1126/sciadv.abm5713.

Jautzy, J.J., Douglas, P.M.J., Xie, H., Eiler, J.M., and Clark, I.D., 2021, CH_4 isotopic ordering records ultra-slow hydrocarbon biodegradation in the deep subsurface: Earth and Planetary Science Letters, v. 562, https://doi.org/10.1016/j.epsl.2021.116841.

Kniemeyer, O., et al., 2007, Anaerobic oxidation of short-chain hydrocarbons by marine sulphate-reducing bacteria: Nature, v. 449, p. 898–901, https://doi.org/10.1038/nature06200.

Lalk, E., Pape, T., Gruen, D.S., Kaul, N., Karolewski, J.S., Bohrmann, G., and Ono, S., 2022, Clumped methane isotopologue-based temperature estimates for sources of methane in marine gas hydrates and associated vent gases: Geochimica et Cosmochimica Acta, v. 327, p. 276–297, https://doi.org/10.1016/j.gca.2022.04.013.

Lin, Y.T., Tu, T.H., Wei, C.L., Rumble, D., Lin, L.H., and Wang, P.L., 2018, Steep redox gradient and biogeochemical cycling driven by deeply sourced fluids and gases in a terrestrial mud volcano: FEMS Microbiology Ecology, v. 94, https://doi.org/10.1093/femsec/fiy171.

Liu, J., et al., 2023, Reversibility controls on extreme methane clumped isotope signatures from anaerobic oxidation of methane: Geochimica et Cosmochimica Acta, v. 348, p. 165–186, https://doi.org/10.1016/j.gca.2023.02.022.

Milkov, A.V., 2011, Worldwide distribution and significance of secondary microbial methane formed during petroleum biodegradation in conventional reservoirs: Organic Geochemistry, v. 42, p. 184–207, https://doi.org/10.1016/j.orggeochem.2010.12.003.

Milkov, A.V., and Etiope, G., 2018, Revised genetic diagrams for natural gases based on a global dataset of >20,000 samples: Organic Geochemistry, v. 125, p. 109–120, https://doi.org/10.1016/j.orggeochem.2018.09.002.

Mishra, S., Wefers, P., Schmidt, M., Knittel, K., Krüger, M., Stagars, M.H., and Treude, T., 2017, Hydrocarbon degradation in Caspian Sea sediment cores subjected to simulated petroleum seepage in a newly designed Sediment-Oil-Flow-Through system: Frontiers in Microbiology, v. 8, https://doi.org/10.3389/fmicb.2017.00763.

Ono, S., Rhim, J.H., and Ryberg, E.C., 2022, Rate limits and isotopologue fractionations for microbial methanogenesis examined with combined pathway protein cost and isotopologue flow network models: Geochimica et Cosmochimica Acta, v. 325, p. 296–315, https://doi.org/10.1016/j.gca.2022.03.017.

Reeburgh, W.S., 2007, Global methane biogeochemistry, in Keeling, R.F., ed., Treatise on Geochemistry, Volume 4: The Atmosphere: Oxford, Pergamon, 32 p., https://doi.org/10.1016/B0-08-043751-6/04036-6.

Stagars, M.H., Mishra, S., Treude, T., Amann, R., and Knittel, K., 2017, Microbial community response to simulated petroleum seepage in Caspian Sea sediments: Frontiers in Microbiology, v. 8, https://doi.org/10.3389/fmicb.2017.00764.

Stolper, D.A., et al., 2014, Formation temperatures of thermogenic and biogenic methane: Science, v. 344, p. 1500–1503, https://doi.org/10.1126/science.1254509.

Taenzer, L., Labidi, J., Masterson, A.L., Feng, X., Rumble, D., III, Young, E.D., and Leavitt, W.D., 2020, Low $\Delta^{12}CH_2D_2$ values in microbialgenic methane result from combinatorial isotope effects: Geochimica et Cosmochimica Acta, v. 285, p. 225–236, https://doi.org/10.1016/j.gca.2020.06.026.

Thiagarajan, N., Kitchen, N., Xie, H., Ponton, C., Lawson, M., Formolo, M., and Eiler, J., 2020, Identifying thermogenic and microbial methane in deep water Gulf of Mexico Reservoirs: Geochimica et Cosmochimica Acta, v. 275, p. 188–208, https://doi.org/10.1016/j.gca.2020.02.016.

Turner, A.C., Pester, N.J., Bill, M., Conrad, M.E., Knauss, K.G., and Stolper, D.A., 2022, Experimental determination of hydrogen isotope exchange rates between methane and water under hydrothermal conditions: Geochimica et Cosmochimica Acta, v. 329, p. 231–255, https://doi.org/10.1016/j.gca.2022.04.029.

Wang, D.T., et al., 2015, Nonequilibrium clumped isotope signals in microbial methane: Science, v. 348, p. 428–431, https://doi.org/10.1126/science.aaa4326.

Whiticar, M.J., 1999, Carbon and hydrogen isotope systematics of bacterial formation and oxidation of methane: Chemical Geology, v. 161, p. 291–314, https://doi.org/10.1016/S0009-2541(99)00092-3.

Xie, H., Dong, G., Formolo, M., Lawson, M., Liu, J., Cong, F., Mangenot, X., Shuai, Y., Ponton, C., and Eiler, J., 2021, The evolution of intra- and inter-molecular isotope equilibria in natural gases with thermal maturation: Geochimica et Cosmochimica Acta, v. 307, p. 22–41, https://doi.org/10.1016/j.gca.2021.05.012.

Young, E.D., 2019, A two-dimensional perspective on CH_4 isotope clumping: Distinguishing process from source, in Orcutt, B.N., et al., eds., Deep Carbon: Past to Present: Cambridge, UK, Cambridge University Press, p. 388–414, https://doi.org/10.1017/9781108677950.013.

Young, E.D., et al., 2017, The relative abundances of resolved $^{12}CH_2D_2$ and $^{13}CH_3D$ and mechanisms controlling isotopic bond ordering in abiotic and biotic methane gases: Geochimica et Cosmochimica Acta, v. 203, p. 235–264, https://doi.org/10.1016/j.gca.2016.12.041.

Zengler, K., Richnow, H.H., Rosselló-Mora, R., Michaelis, W., and Widdel, F., 1999, Methane formation from long-chain alkanes by anaerobic microorganisms: Nature, v. 401, p. 266–269, https://doi.org/10.1038/45777.

Zhang, N., Snyder, G.T., Lin, M., Nakagawa, M., Gilbert, A., Yoshida, N., Matsumoto, R., and Sekine, Y., 2021, Doubly substituted isotopologues of methane hydrate ($^{13}CH_3D$ and $^{12}CH_2D_2$): Implications for methane clumped isotope effects, source apportionments and global hydrate reservoirs: Geochimica et Cosmochimica Acta, v. 315, p. 127–151, https://doi.org/10.1016/j.gca.2021.08.027.

Zhou, Z., et al., 2022, Non-syntrophic methanogenic hydrocarbon degradation by an archaeal species: Nature, v. 601, p. 257–262, https://doi.org/10.1038/s41586-021-04235-2.

Printed in the USA